To be published to
Nuclear Physics A

ISTITUTO NAZIONALE DI FISICA NUCLEARE
Laboratori Nazionali di Frascati

LNF-81/60(P)
16 Ottobre 1981

F. Balestra, M.P. Bussa, L. Busso, R. Garfagnini, C. Guaraldo, A. Maggiora, D. Panzieri, G. Piragino and R. Scrimaglio: POSITIVE PION-NUCLEUS ELASTIC BACKWARD SCATTERING FROM ^{12}C AT 30, 40 AND 50 MeV.

Servizio Documentazione
dei Laboratori Nazionali di Frascati

INFN Laboratori Nazionali di Frascati
Servizio Documentazione

LNF-81/60(P)
16 Ottobre 1981

POSITIVE PION-NUCLEUS ELASTIC BACKWARD SCATTERING FROM ^{12}C AT 30, 40 AND 50 MeV.

C.Guaraldo, A.Maggiora, R.Scrimaglio
INFN, Laboratori Nazionali di Frascati, Frascati (Italy)

F.Balestra, M.P.Bussa, L.Busso, R.Garfagnini, D. Panzieri, G. Piragino
Istituto di Fisica dell'Università di Torino, and INFN, Sezione di Torino, Torino (Italy)

Summary.

The elastic scattering of positively charged pions from ^{12}C at 160°, 168° and 176° has been measured at 29, 38, 44, 50 and 56 MeV. The experimental apparatus consisted of a magnetic spectrometer with a helium-filled selfshunted streamer chamber for identifying scattering events by detecting both the incident and scattered pion tracks. The new data do complete the existing angular distributions at 30, 40 and 50 MeV, thus allowing for a full comparison to recent second order calculations. An analysis of the role played by the various higher order effects, by investigating both energy and angular dependencies, can be performed.

Low energy pion-nucleus scattering has been stimulating a great amount of work in these recent years. The field has been proving to be a significant area for informations about mechanisms of pion-nucleus interaction. Large and significative differences between experiments and simple theoretical predictions have been exhibited.

In the energy region near the πN(3-3) resonance all kind of different processes can be described in terms of a simple optical potential, which is of the form of the nuclear density ϱ multiplied by the elementary pion-nucleon off-shell T-matrix. As a consequence of the dominance of the resonance, the optical potential is highly absorbitive, so that the mean free path of a pion is small and, consequently, most of scattering takes place on the nuclear surface.

For T_π = 50 MeV the pion mean free path is about 5 fms, the nucleus becomes more transparent to the pion and the pion has more chances to sample the interior region of the nucleus, as a probe of the properties of nuclear matter. However, first order optical potentials, derived from the free πN amplitudes, have shown to be inadequate in describing low energy pion-nucleus scattering. Higher order effects, such as true pion absorption and two nucleon correlations - nucleon binding, Pauli effects, short range correlations - must play an important role and have to be included in the model. Although is still object of debating as to how these second order

effects should be included, there is a general agreement about their importance for even a qualitative description of the data.

Several measurements of low energy pion nucleus elastic scattering have already been published, covering angular distributions up to 160°[1-12]. This paper presents backward measurements for the elastic scattering of π^+ from ^{12}C at energies of 29, 38, 44, 50 and 56 MeV. We have previously published π^+ elastic backward scattering data from ^{12}C at 29 MeV[5]. These earlier data are summarized here for completeness. The methods used in this experiment are substantially different from those used in other experiments. In our experimental apparatus the large and backward angles measurements are carried simultaneously for all energies, avoiding any relative error among different runs. Moreover, the present data allow to define the general trend of the elastic angular distributions at backward angles at 30, 40 and 50 MeV. In such a way it becomes possible to make a complete comparison to most popular recent second order calculations[13-15]. In particular, it seems possible to perform a qualitative analysis of the role played by the various higher order effects, by investigating energy and angular dependencies.

The experimental data were taken at the LEALE pion beam facility of Laboratori Nazionali di Frascati[16]. The pion beam is photoproduced on a graphite target by a bremsstrahlung beam obtained, in turn, by the electron beam of the Frascati linac on a tungsten radiator.

The pion channel delivers about 10^5 pions per second at a nominal energy of 57.3 MeV, corresponding to an energy of 50.0 MeV at the centre of the target, with a 32 μA at 320 MeV primary electron mean current. In this experiment we accepted a beam with a $\pm$ 15% momentum distribution around the nominal value, in order to carry out simultaneously measurements at different energies.

The experimental set up has been described in detail elsewhere[17-18]. It consisted of a magnetic spectrometer with a helium-filled self-shunted streamer chamber, for identifying scattering events by detecting both the incident and scattered pion tracks.

A hodoscope of thin scintillation counters defined the number of pions deflected by the magnet and impinging on the experimental target. The target was a pressed natural carbon sheet of 99.9% purity, and a measured density, for a total thickness of 553 mg/cm^2. Pions scattered in the backward direction by the target were deflected with opposite curvature and were detected by two large scintillation counters in coincidence with the hodoscope.

The coincidence triggered the high voltage pulse on the streamer chamber and the commands of two cameras, thus allowing to photograph the scattering events.

The pion flux at the target position was reduced to about 10^2 pions per second, in order to avoid the pile-up of tracks on the photographs and to reduce the background in the counter telescope.

The pion dose was corrected for the counter efficiencies and for contamination of the pion beam due to positrons and decay muons. The contamination was measured by a time of flight technique, with a 1.34 m long basis, at 15.8, 27.5, 30.4 and 33.1 MeV central target energies. In these measurements the momentum band accepted was $\pm$1%.

The evaluation of the detection efficiency of the apparatus as a function of incident and scattered pion energies and of the scattering angle was performed by means of a Monte Carlo calculation. The distributions of particles on the target and on the backward scintillation counters were compared with the experimental ones and found in quite satisfactory agreement.

Tracks reconstruction and data analysis procedure were carried out with the codes SC 180 and SOLID, respectively, as described in refs. (17,19). The resolution of a track depends on the energy lost in the target and is a function of a number of parameters: track lenght in the streamer chamber, number of measured points along a track, uncertainty in the measuring points, value of the curvature radius. An overall energy resolution (FWHM) $\Delta T/T \simeq$ 2.5% (sufficient for clearly selecting the elastic scattering) was obtained for a 300 mm average

track lenght, 15 measured points, ± 0.2 mm uncertainty in locating points, curvature radius 1175 mm (corresponding to 50.9 MeV pion kinetic energy at the middle of the chamber). The scattering angle could be obtained with negligible errors of reconstruction (±0.5) and multiple scattering in the target.

The events were statistically assigned to the elastic or to the inelastic channels by evaluating the normalized probability to belong to the various processes through a computer routine (LEVEL), which took advantage of angular and energy informations and also corrected data for the energy lost in the target by ionization.

After correcting for the detection efficiency of the apparatus, i.e. for the effective solid angle, a total of 1038 backward scattering events was used to evaluate the elastic cross sections. The data were grouped into four energy intervals: 38 ± 3 MeV, 44 ± 3 MeV, 50 ± 3 MeV, 56 ± 3 MeV and in three (two for 38 MeV data) angular bins: 160° ± 4°, 168° ± 4°, 176° ±4°. The eleven corresponding elastic differential cross sections are listed in Table I.

TABLE I

(π^+, ^{12}C) elastic differential cross section (mb/sr) c.m.

T_π^{lab} (MeV) / $\theta_\pi^{c.m.}$ (deg)	38 ± 3	44 ± 3	50 ± 3	56 ± 3
160°. 3 ± 4°		5.99 ± 1.56	6.28 ± 2.45	2.01 ± 2.01
168°. 2 ± 4°	8.47 ± 3.24	7.95 ± 1.77	4.83 ± 1.27	4.26 ± 1.88
176°. 1 ± 4°	6.79 ± 3.15	7.84 ± 1.76	5.94 ± 1.50	2.63 ± 1.44

The error quoted on the cross sections were deduced from propagation of three main sources: statistical errors on incoming dose and backward events; errors on the coefficients which define the effective solid angle for each event; errors on the effective nuclei target numbers. The large errors at lower energies reflect the poor statistics in that energy region of the incident spectrum.

In Fig.1 we present backward angle data for the elastic scattering of π^+ from ^{12}C at energies of 30, 40 and 50 MeV. We have previously published π^+ elastic scattering data from ^{12}C at backward angles at 29 MeV[5]. These earlier data are summarized here for completeness.

The previously obtained backward angle data at 29 MeV are reported together with the old measurements of Marshall et al.[1], with the angular distribution of Jonhson et al.[3], and with the angular distribution of Preedom et al.[6].

The 40 MeV backward angle data are shown together with the angular distributions of Johnson et al.[3] and of Blecker et al.[7].

The present 50 MeV large angle data do complete the angular distributions obtained through the value of Dytman et al.[12], those of Johnson et al.[3] and those of Moinester et al.[11].

As for the 160° value at 30 MeV of this experiment and the corresponding one in the distribution of Johnson et al.[3], the new 50 MeV measurement at 160° is in agreement, within the error, with data of other experiments: in particular with the result of Moinester et al.[11]. To stress the significance of this fact, we

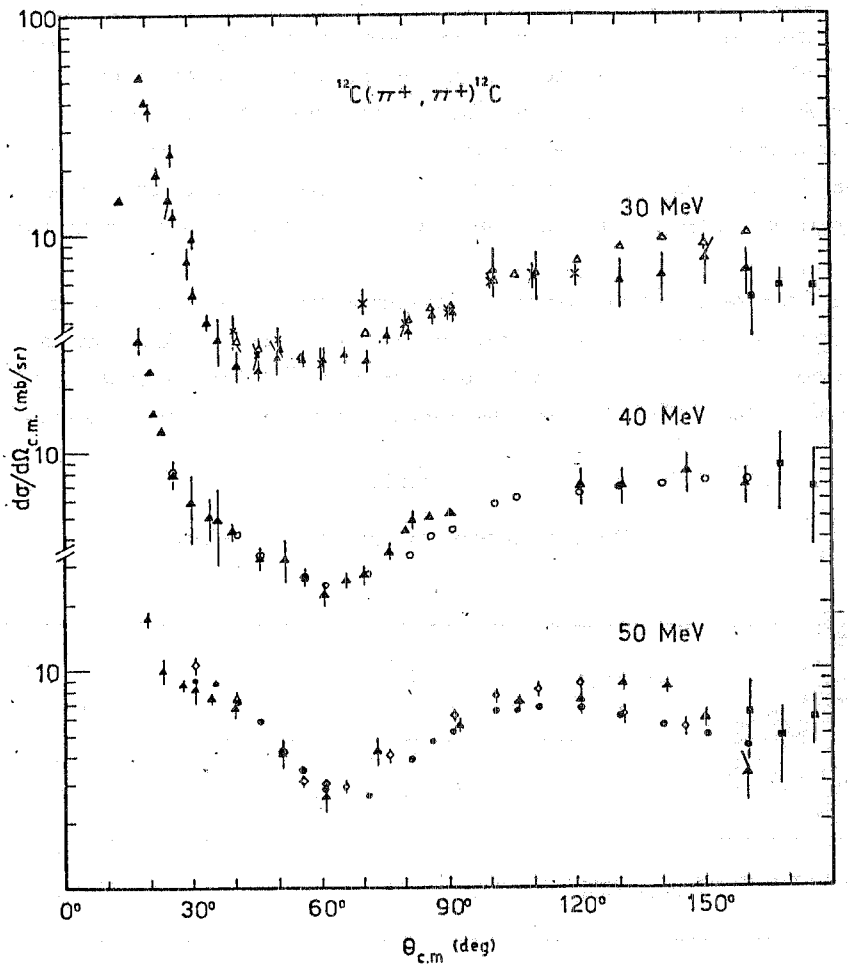

Fig. 1 - Experimental differential cross sections for the elastic scattering of π^+ from ^{12}C at 30, 40 and 50 MeV. The black squares are present data at 29, 38 and 50 MeV, respectively. The open triangles are from ref. 6 at 30.3 MeV. The black triangles are from ref. 3 at 28.4, 38.6 and 48.9 MeV, respectively. The x's are from ref. 1 at 30 MeV. The open circles are from ref. 7 at 40 MeV. The black circles are from ref. 11 at 49.9 MeV. The open rhombs are from ref. 12 at 50 MeV.

recall that the agreement is found between experiments employing completely different experimental techniques. In the work of Dytman et al.[12] one detector system was used at different angles to detect the elastically scattered pions. This detector consisted of three delay-line read out proportional chambers, to determine the trajectory of the pion, and two crystal intrinsic germanium detectors, to stop the pion and provide total energy information. They used a CH_2 target and normalized their data to measured π^+p cross sections[20]. In the work of Johnson et al.[3] two detector systems were used simultaneously. Each system consisted of three plastic scintillators, the first two defining the solid angle subtended by the telescope and the third providing total energy informations. In the work of Moinester et al.[11], in order to minimize the relative error between differential cross sections measured at various angles, a ten-detector array of plastic scintillators was used, allowing to measure a complete angular distribution in two runs. The absolute normalization was checked by comparison of measured values of the differential cross section for π^+p scattering with those measured by Bertin et al.[20].

In our experimental apparatus the backward angle mesurements at various energies are carried out

simultaneously, avoiding any relative error among different runs. The pion flux is measured with the in-beam counter telescope discussed above. The incident energy spectrum, and therefore the effective dose in every energy bin, is corrected for a calculated detection efficiency, whose check compares favourably with the measured track distributions.

The present data allow for defining the trends of the angular distributions at backward angle at 40 and 50 MeV, after the early one obtained at 30 MeV. It seems possible to conclude that the general behaviour of the three angular distributions appears to be flat at 180 degrees, with a weak negative derivative, especially at 50 MeV. The conclusion is in disagreement with the net descending behaviour suggested by the previous data.

Recent second order calculations can be compared with the new backward angle data. In Figg. 2, 3 and 4 the experimental distributions at 30, 40 and 50 MeV are compared with the theoretical predictions obtained by two potentials of current interest: the second order optical potential of Landau and Thomas[13] and the phenomenological potential of Stricker, Mc Manus and Carr[15], whose parameters are deduced through a fit to pionic atom data.

The first calculation, in an effort to produce as complete a theoretical description for low energy π-nucleus scattering as possible with a first order optical potential, includes both a detailed analysis about the sensitivity of the results to πN phase shifts used and the effects of the Pauli exclusion principle on the struck nucleon.

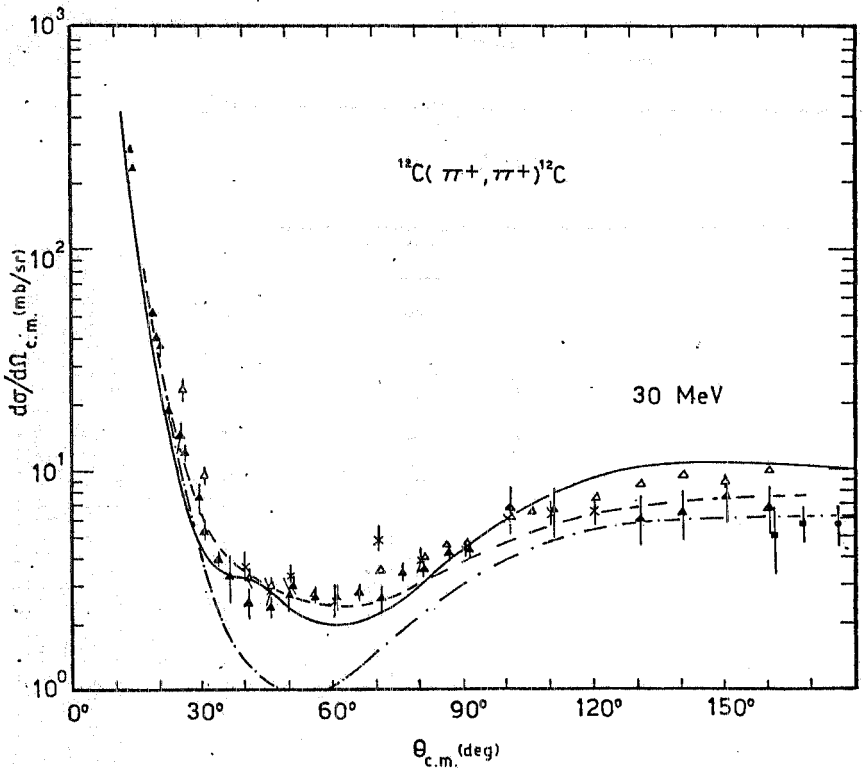

Fig. 2 - The backward data at 29 MeV of this experiment (black squares) compared to the calculations of Landau and Thomas[13] (solid line), Stricker, Mc Manus and Carr[15] (dashed curves) and Cannata[7] (dot dashed curve). Angular distributions from ref.3 at 28.4 MeV (black triangles), from ref.6 at 30.3 MeV (open triangles) and from ref.1 at 30 MeV (x's) are also shown.

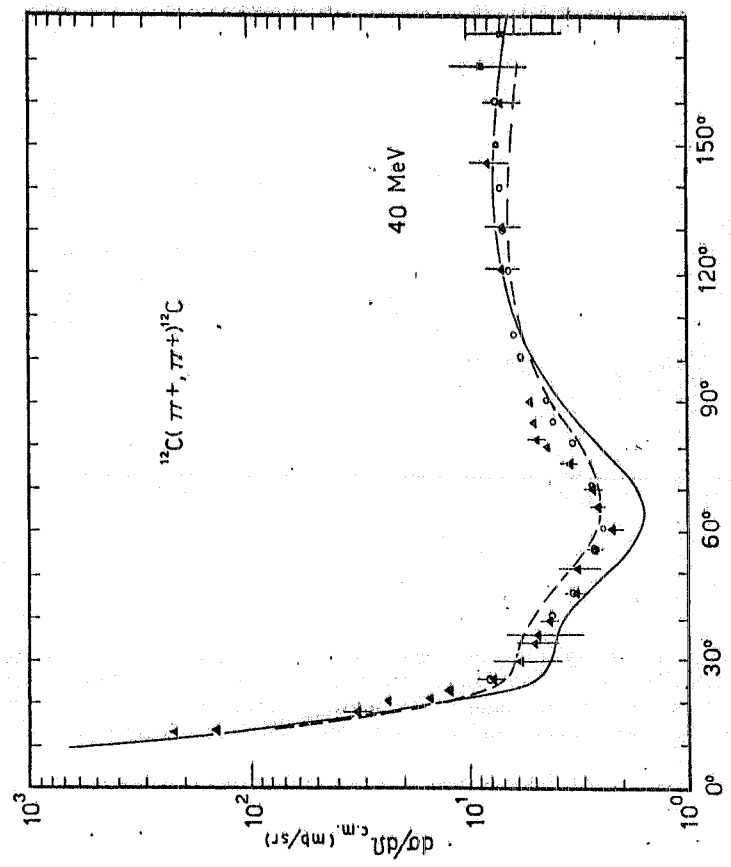

Fig. 3 - The backward data at 38 MeV of this experiment (black squares) compared to the calculations of Landau[13] and Thomas[13] (solid line) and Stricker, Mc Manus and Carr[13] (dashed line). Angular distributions from ref.3 at 38.6 MeV (black triangles) and from ref.7 at 40 MeV (open circles) are also shown.

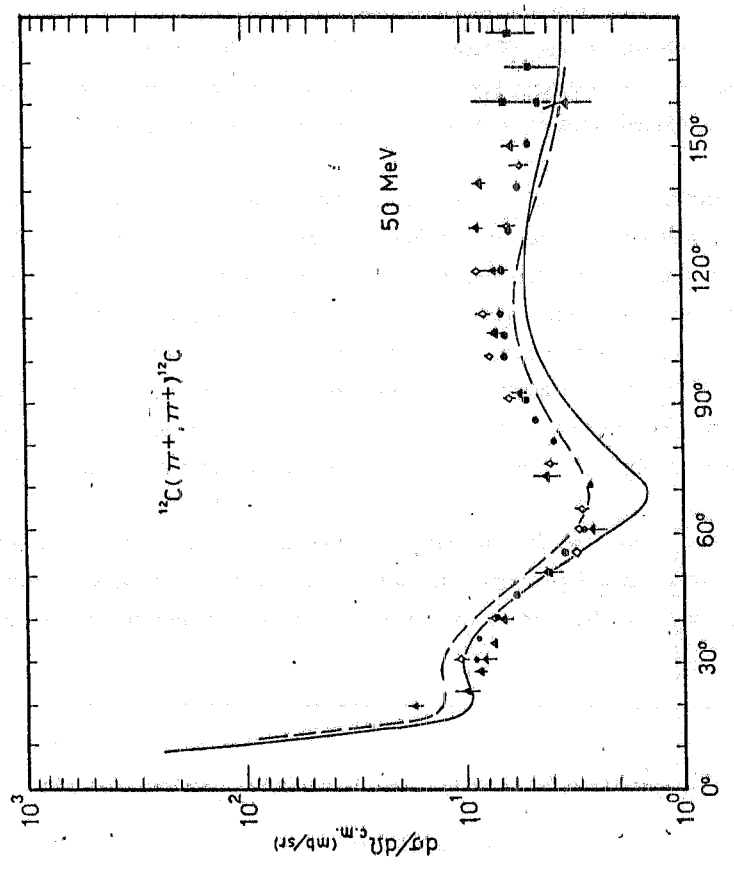

Fig. 4 - The backward data at 50 MeV of this experiment (black squares) compared to the calculations of Landau and Thomas[13] (solid line) and Stricker, Mc Manus and Carr[13] (dashed line). Angular distributions from ref.3 at 48.9 MeV (black triangles), from ref.11 at 49.9 MeV (black circles) and from ref.12 at 50 MeV (open rhombs) are also shown.

Among the new phenomena that seems to play an important role in the lower energy regime, an outstanding feature at essentially zero energy is that the energy levels of pionic atoms have finite widths, because pions can be absorbed by nuclei. The true pion absorption is the only exotic effect included in this theory which is not implicit in the potential model, but taken into account in a semiphenomenological way, through a second order term proportional to $\varrho^2(r)$ and whose magnitude matches the pionic atom results[21]. The inclusion of finite-range interactions, nucleon recoil and three-body binding effects was also considered.

We will now analyze the role of true pion absorption in different angular and energy regions.

In the comparison with experimental data, true pion absorption is especially important at 30 MeV and less at 50 MeV. This is particularly clear in the Coulomb-nuclear interference region that, at these low energies, extends over a broader and more accessible angular region than at higher energies[22]. When the energy is lowered to 30 MeV, where the Coulomb and πN P-wave minimum coalesce, the first order potential is completely inadequate to fill the minimum[13]. If the effect of two-nucleon absorption is now included in the Landau and Thomas potential, the cross section is raised and the minimum gets filled, demonstrating the crucial role played at 30 MeV both from Coulomb-nuclear interference and from true pion absorption. This evidence becomes less challenging as energy increases. All this is shown in the quoted figures (solid lines): even if the general shapes of the experimental distributions are only partially reproduced, the forward region (up to 60°) is fitted at 30 MeV, partially at 40 MeV and with less agreement at 50 MeV, where true pion absorption has a decreased relevance.

Large and backward angles situation appears quite different. As already we pointed out in our previous work[5], the most challenging effect at backward in the very low energy region ($\lesssim$ 30 MeV) seems to be nucleon-nucleon correlations, described by the Ericson-Ericson-Lorentz-Lorenz effect[23]. The role played by this effect at backward is shown in Fig. 2. The dot dashed curve is the result of a calculation[5] using the only EELL effect in the original gradient potential: the large and backward angle experimental values at 30 MeV are very well reproduced by the model. On the contrary, Landau and Thomas calculation misses our data at 30 MeV (Fig. 2), it is in agreement with our experiment and with large angle distributions at 40 MeV (Fig. 3), while, at 50 MeV, it largerly underestimates the cross sections, with a too strong descending behaviour (Fig. 4). Since the EELL correction is the only effect not included in this model, the substantial disagreement at large angle, with the exception of the 40 MeV data, might be interpreted as an indirect confirm of its importance.

However, other considerations might suggest the necessity of neglecting the effect in this particular model, making less clear a definite conclusion. When a zero range πN interaction is used, the EELL effect plays an essential role in reducing the off-shell dependence of the π-nucleus cross section. But, in presence of fairly long range πN interactions, as in the Landau and Thomas' model, the off-shell sensitivity is already small and nucleon-nucleon correlations ought to produce only a small correction[24].

Moreover, as far as, in particular, the 50 MeV data are concerned, Landau and Thomas observe that even using Salomon's recent phase shift tabulations[25], the level of inadequatity of isospin $\frac{1}{2}$ πN data is such that there is at least a 20% (probably more at 50 MeV) uncertainty in the theory!

Comparison of now complete angular distributions with the calculations of Stricker, Mc Manus and Carr[15] allows for further considerations on low energy pion-nucleus elastic scattering. This work calculates the pion-nucleus scattering cross section using the optical parameters which fit the pionic atom data. Basically, the data determine only four parameters of the optical potential, the others are taken from theory. True pion absorption is esplicitly taken into account and it is, as usually, parametrized in terms of the nuclear density. Moreover, the Ericson-Ericson-Lorentz-Lorenz effect is included, together with terms in $\nabla^2\varrho$ and $\nabla^2\varrho^2$, following Thies[26]. These terms arise from the so called "angle-transformation", i.e. the transformation of the $\vec{k}.\vec{k}'$ factor in the p-wave term of the potential from the pion-nucleon centre of mass system to the pion-nucleus centre of mass system ($\vec{k}$ is the momentum of the pion in this last reference system).

Figures 2, 3 and 4 (dashed curves) show an agreement of Stricker, Mc Manus and Carr calculations to experimental distributions, at least as far as the general trends are concerned. Let's examine large and backward angle data. The $\nabla^2\rho$ term in the potential increases backward angle scattering, improving the fit to our data. Moreover, the role of nuclear correlations in this angular region, through the EELL effect, can now be supported by new argomentations. We recall that the EELL effect is usually taken into account modifying the p-wave term in the classical form of the optical potential[14] by multiplying it for the so called Ericson-Ericson factor

$$L(r) = \left\{ 1 + \frac{4}{3} \lambda \left[c(r) + \frac{C_0}{p_2} \rho^2 \right] \right\}^{-1} ,$$

where the parameter λ is related to the nucleon correlation function and the other symbols are those of ref. (14).

This factor has the effect of weakening the p-wave attraction to an extent just determined by the correlation parameter λ, by inhibiting second order scattering if the pion-nucleon p-wave interaction is of short range enough, as shown by Eisenberg, Hüfner and Moniz[27]. If inhibition is complete, $\lambda = 1$. It seems then possible to conclude that the lower energy is, the weaker p-wave nuclear attraction will be and therefore more evident the EELL weakening effect will appear. On the other side, the higher energy is, the stronger p-wave attraction will be and less effective the effect will result.

Our experimental data seem to support this kind of conclusions, since the agreement with potentials which take into account NN correlations is quite satisfactory at 30 and 40 MeV (Fig. 2: dashed and dot-dashed curves) and Fig. 3 (dashed curve), while the agreement is less good at 50 MeV (Fig. 4).

Also true pion absorption energy and angular dependencies can be put in further evidence. Low energy elastic scattering from light nuclei is principally sensitive to the interferences between Coulomb scattering, nuclear scattering from the repulsive s-wave part of the optical potential and nuclear scattering from the attractive velocity dependent p-wave part. The 50 MeV distribution shows more interference pattern than the 30 MeV one (see Fig.1), as the effect of the interaction of the Coulomb potential with a velocity dependent nuclear potential. In fact,the p-wave attraction increases in going from 30 to 50 MeV and the interference increases.

Moreover, in this context, true pion absorption plays an essential role at low energy. The absorbitive part of the optical potential heavily damps any interference structure at 30 MeV, while the effect is not so strong at higher energies, allowing for the presence of an interference pattern at 50 MeV. This general trend is riproduced by the model at all energies, as shown in Figg. 2, 3 and 4 (dashed curves).

These conclusions are recalled in Fig. 5, in which two fits to the data, from ref. (15), are presented. The dashed curves are obtained by the current Stricker, Mc Manus and Carr potential. The dotted curves are obtained with "less absorption" parameters. As also stressed by the authors, while the agreement at 40 and 50 MeV is satisfactory, the reduced absorption gives a poorer fit in the forward angular region at 30 MeV, so confirming the previous considerations.

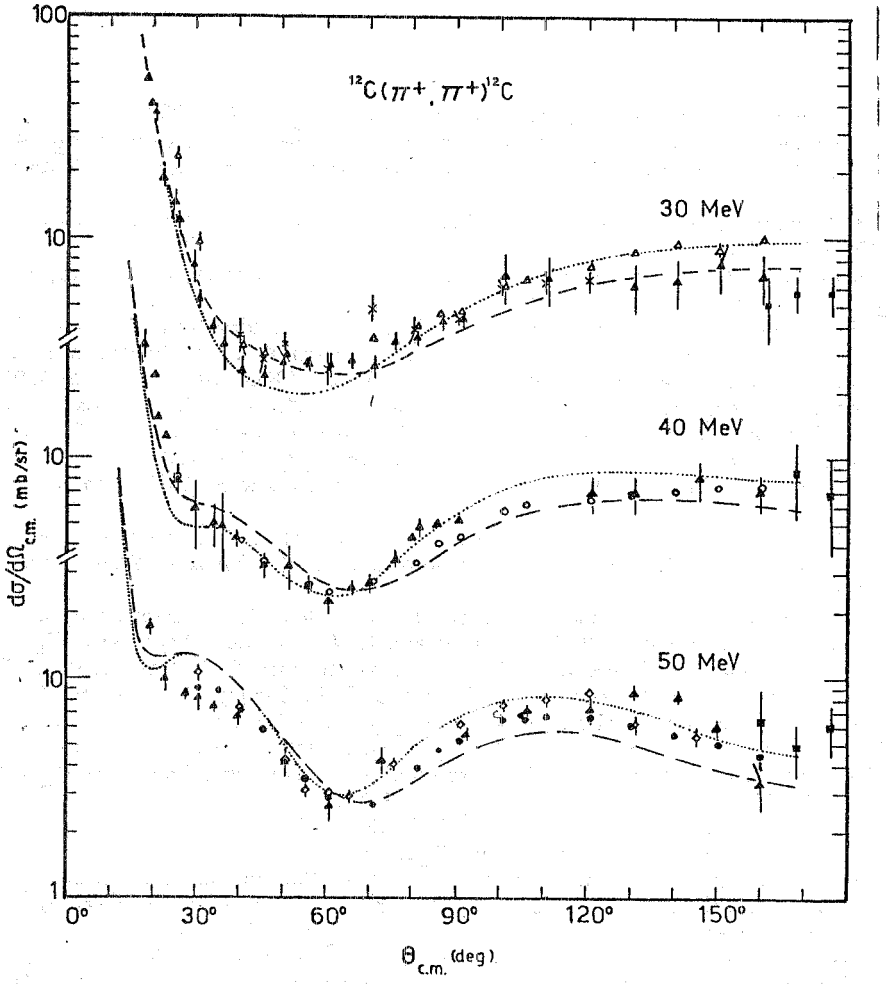

Fig. 5 - The role of true pion absorption in low energy pion-nucleus elastic scattering. The curves are calculations of Stricker, Mc Manus and Carr from ref.15. The dashed curve is obtained by the current Stricker, Mc Manus and Carr potential. The dotted curve is obtained through a reduction in absorption parameters of the same low energy optical potential. The experimental points are those of Fig.1.

REFERENCES

(1) J. F. Marshall, M. E. Nordberg Jr. and R. L. Burman, Phys. Rev. C1, 1685 (1970).
(2) H. Dollard, K. L. Erdman, R. R. Johnson, T. Masterson and P. Walden, Phys. Letters 63B, 416 (1976).
(3) R. R. Johnson, T. G. Masterson, K. L. Erdman, A. W. Thomas and R. H. Landau, Nuclear Phys. A296, 444 (1978).
(4) R. R. Johnson, B. Bassalleck, K. L. Erdman, B. Gyles, T. Marks, T. Masterson, D. R. Gill and C. Sabev, Phys. Letters 78B, 560 (1978).
(5) C. Guaraldo, A. Maggiora, R. Scrimaglio, F. Balestra, L. Busso, R. Garfagnini, G. Piragino and F. Cannata, Phys. Letters 80B, 203 (1979).
(6) B. M. Preedom, S. H. Dam, C. W. Darden III, R. D. Edge, D. J. Malbrough, T. Marks, R. L. Burman, M. Hamm, M. A. Moinester, R. P. Redwine, M. A. Yates, F. E. Bertrand, T. P. Cleary, E. E. Gross, N. W. Hill, C. A. Ludemann, M. Blecher, K. Gotow, D. Jenkins and F. Milder, Phys. Rev. C23, 1134 (1981).
(7) M. Blecher, K. Gotow, D. Jenkins, F. Milder, F. E.Bertrand, T. P.Clearly, E. E. Gross, C. A. Ludemann, M. A. Moinester, R. L. Burman, M. Hamm, R. P. Redwine, M. YatesWilliams, S. Dam, C. W. Darden III, R. D. Edge, D. J. Malbrough, T. Marks and B. M. Preedom, Phys. Rev. C20, 1884 (1079).
(8) J. F. Amann, P. D. Barnes, M. Doss, S. A. Dytman, R. A. Eisenstein and A. C. Thompson, Phys. Rev. Letters 35, 429 (1975).
(9) S. A. Dytman, J. F. Amann, P. D. Barnes, J. N. Craig, K. G. R.Doss, R. A. Eisenstein, J. D. Sherman, W. R. Wharton, R. J. Peterson, G. R. Burleson, S. L. Verbeck and H. A. Thiessen, Phys. Rev. Letters 38, 1059 (1977); 39, 53(E) (1977).
(10) S. A. Dytman, J. F. Amann, P. D. Barnes, J. N. Craig, K. G. R.Doss, R. A. Eisenstein, J. D. Sherman, W. R. Wharton, G. R. Burleson, S. L. Verbeck, R. J. Peterson and H. A. Thiessen, Phys. Rev. C18, 2316 (1978).
(11) M. A. Moinester, R. L. Burman, R. P. Redwine, M. A. Yates-Williams, D. J. Malbrough, C. W. Darden, R. D. Edge, T. Marks, S. H. Dam, B. M. Preedom, F. E. Bertrand, T. P. Cleary, E. E. Gross, C. A. Ludemann, M. Blecher, K. Gotow, D. Jenkins and F. Milder, Phys. Rev. C18, 2678 (1978).
(12) S. A. Dytman, J. F. Amann, P. D. Barnes, J. N. Craig, K. G. R.Doss, R. A. Eisenstein, J. D. Sherman, W. R. Wharton, G. R. Burleson, S. L. Verbeck, R. J. Peterson and H. A. Thiessen, Phys. Rev. C19, 971 (1979).
(13) R. H. Landau and A. W. Thomas, Nuclear Phys. A302, 461 (1978).
(14) K. Stricker, H. Mc Manus and J. A. Carr, Phys. Rev. C19, 929 (1979).
(15) K. Stricker, J. A. Carr and H. Mc Manus, Phys. Rev. C22, 2043 (1980).
(16) R. Barbini, S. Faini, C. Guaraldo, C. Schaerf and R. Scrimaglio, Nuclear Instr. and Meth. 105, 515 (1972).
(17) F. Balestra, L. Busso, R. Garfagnini, G. Piragino, R. Barbini, C. Guaraldo, R. Scrimaglio, I. V. Falomkin, M. M. Kulyukin and Yu. A. Shcherbakov, Nuclear Instr. and Meth. 119, 347 (1974).
(18) F. Balestra, L. Busso, R. Garfagnini, G. Perno, G. Piragino, R. Barbini, C. Guaraldo, R. Scrimaglio, I. V. Falomkin, M. M. Kulyukin, G. B. Pontecorvo and Yu A. Shcherbakov, Nuclear Instr. and Meth. 125, 157 (1975).
(19) F. Balestra, L. Busso, R. Garfagnini, G. Piragino, R. Barbini, C. Guaraldo and R. Scrimaglio, Nuovo Cimento 33A, 281 (1976).
(20) P. Y. Bertin, B. Coupat, A. Hivernat, D. B. Isabelle, J. Duclos, A. Gerard, J. Miller, I. Morgenstern, J. Picard, P. Vernin and R. Powers, Nuclear Phys. B106, 341 (1076).
(21) J. Hüfner, Phys. Report 21C, 1 (1975).
(22) F. Binon, P. Duteil, J. -P. Garron, J. Görres, L. Hugon, J. -P. Peigneux, C. Schmit, M. Spighel and J. -P. Stroot, Nuclear Phys. B17, 168 (1970).
(23) M. Ericson and T. E. O. Ericson, Ann. of Phys. 36, 323 (1966).
(24) R. H. Landau and F. Tabakin, Nuclear Phys. A231, 445 (1974).
(25) M. Salomon, TRIUMF Report TRI-74-2 (1974).
(26) M. Thies, Phys. Letters 63B, 43 (1976).
(27) J. M. Eisenberg, J. Hüfner and E. J. Moniz, Phys. Letters 47B, 381 (1973).